



Published in final edited form as:

*Science*. 2016 April 29; 352(6285): 604–607. doi:10.1126/science.aac8167.

## Broken detailed balance at mesoscopic scales in active biological systems

Christopher Battle<sup>#1,2</sup>, Chase P. Broedersz<sup>#2,3,4</sup>, Nikta Fakhri<sup>#1,2,5</sup>, Veikko F. Geyer<sup>6</sup>, Jonathon Howard<sup>6</sup>, Christoph F. Schmidt<sup>1,2,†</sup>, Fred C. MacKintosh<sup>2,7,†</sup>

<sup>1</sup>Drittes Physikalisches Institut, Georg-August-Universität, 37077 Göttingen, Germany <sup>2</sup>The Kavli Institute for Theoretical Physics, University of California, Santa Barbara, CA 93106, USA <sup>3</sup>Arnold-Sommerfeld-Center for Theoretical Physics and Center for NanoScience, Ludwig-Maximilians-Universität München, Theresienstrasse 37, D-80333 München, Germany <sup>4</sup>Lewis–Sigler Institute for Integrative Genomics and Joseph Henry Laboratories of Physics, Princeton University, Princeton, NJ 08544, USA <sup>5</sup>Department of Physics, Massachusetts Institute of Technology, Cambridge, MA 02139, USA <sup>6</sup>Department of Molecular Biophysics and Biochemistry, Yale University, New Haven, CT, USA <sup>7</sup>Department of Physics and Astronomy, Vrije Universiteit, Amsterdam, Netherlands

# These authors contributed equally to this work.

### Abstract

Systems in thermodynamic equilibrium are not only characterized by time-independent macroscopic properties, but also satisfy the principle of detailed balance in the transitions between microscopic configurations. Living systems function out of equilibrium and are characterized by directed fluxes through chemical states, which violate detailed balance at the molecular scale. Here we introduce a method to probe for broken detailed balance and demonstrate how such nonequilibrium dynamics are manifest at the mesoscopic scale. The periodic beating of an isolated flagellum from *Chlamydomonas reinhardtii* exhibits probability flux in the phase space of shapes. With a model, we show how the breaking of detailed balance can also be quantified in stationary, nonequilibrium stochastic systems in the absence of periodic motion. We further demonstrate such broken detailed balance in the nonperiodic fluctuations of primary cilia of epithelial cells. Our analysis provides a general tool to identify nonequilibrium dynamics in cells and tissues.

---

When a system reaches thermodynamic equilibrium, its properties become stationary in time, which requires a net balance between rates of transitions into and out of any particular microstate of the system. Systems in thermodynamic equilibrium, however, are known to be balanced in an even stronger way. They obey detailed balance, in which transition rates between any two microstates are pairwise balanced (Fig. 1A). This means there can be no net flux of transitions anywhere in the phase space of system states. This principle was identified and used by Ludwig Boltzmann in his pioneering development of statistical mechanics, the microscopic basis for thermodynamics (1). In contrast, living systems

---

<sup>†</sup>Corresponding author. fcmack@gmail.com (F.C.M.); christoph.schmidt@phys.uni-goettingen.de (C.F.S.).

operate far from equilibrium, and molecular-scale violations of detailed balance lie at the heart of their dynamics. For instance, metabolic and enzymatic processes drive closed-loop fluxes through the system's chemical states (Fig. 1B) (2).

Nonequilibrium driving can boost intracellular transport (3–5), the fidelity of transcription (6), chemotaxis (7, 8), and the accuracy of sensory perception (9, 10). To understand cell function, it is thus important to determine whether particular cellular processes result from nonequilibrium activity, but this can be challenging. For instance, the stochastic nonequilibrium motion of tracer particles or fluorescently labeled proteins in cells is often deceptively similar to that of thermally agitated Brownian particles (3–5, 11). It is unclear, however, to what extent the dynamics at such mesoscopic scales violate detailed balance, even if the system is out of equilibrium. Theoretically, detailed balance can reemerge at large scales for nonequilibrium systems, which break detailed balance at small scales (12). To test for detailed balance and diagnose nonequilibrium dynamics at mesoscopic scales, we introduce a noninvasive approach based on quantifying flux loops (13) in configurational phase spaces of strongly fluctuating stochastic steady-state systems. This should be contrasted with the deterministic dynamics of active swimmers, for which broken detailed balance is evident in the nonreciprocal nature of their motion (14). Moreover, our method is not limited to measuring conformational degrees of freedom, but can also include chemical variables, such as pH or ion concentrations.

We first illustrate this approach on a system displaying unmistakable nonequilibrium motion: a beating flagellum of *Chlamydomonas reinhardtii*. The main mechanical component of eukaryotic flagella is a conserved microtubule structure, the axoneme. Dynein motors drive relative axial sliding of the microtubules composing the axoneme, resulting in periodic beating (15, 16). We isolated and demembrated flagella from *C. reinhardtii* (17, 18) and reactivated the axonemes by addition of adenosine triphosphate (ATP). Figure 1C shows snapshots of the beat cycle acquired by high-speed phase contrast microscopy (movie S1). We decomposed the axoneme shapes into the dynamic normal modes of a finite elastic filament freely suspended in a liquid (19), obtaining amplitudes  $a_1(t)$ ,  $a_2(t)$ ,  $a_3(t)$  for the first three modes (Fig. 1D). From the time series of these amplitudes, we constructed a trajectory in the phase space spanned by the three modes. We discretized this space into a coarse-grained phase space (CGPS) (fig. S1) and determined the probabilities  $p_\alpha$  to be in box  $\alpha$  by temporal averaging (18). The steady-state dynamics are described by net transition rates  $w_{\alpha,\beta} = (N_{\alpha,\beta} - N_{\beta,\alpha})/t_{\text{total}}$  determined by counting the number of transitions between adjacent states  $\alpha$  and  $\beta$  in the time window  $t_{\text{total}}$ . These rates  $w_{\alpha,\beta}$  determine the vector components of the flux  $\vec{j}$  from  $\alpha$  to  $\beta$  (Fig. 1, F and G). In thermodynamic equilibrium, all these fluxes must vanish. By contrast, flux in closed loops is possible in a nonequilibrium steady state. The results of such a probability flux analysis (PFA) for the beating cilium are shown in Fig. 1E, with vector fields indicating the fluxes for the first three modes. Figure 1, F and G, shows the  $a_1 \times a_2$  and  $a_1 \times a_3$  projections of CGPS probability and flux map. The clearly visible flux loops in phase space reflect the nonequilibrium, steady-state dynamics of the beating flagellum, and these fluxes are absent in the equilibrium dynamics of a microtubule (figs. S17 and S18).

The beating flagellum is an obvious nonequilibrium system, driven through its configurations at a defined frequency with relatively little stochasticity (20), resulting in a narrow band of populated states in phase space through which the trajectory cycles unidirectionally. To test our approach on a purely stochastic system, we numerically studied two overdamped, tethered beads at positions  $x_1(t)$  and  $x_2(t)$  coupled by a spring (Fig. 2A). This model system can be driven out of equilibrium by connecting the two beads to different heat baths at temperatures  $T_1$  and  $T_2$ , respectively, leading to heat flux from hot to cold. This minimal model is similar to a class of thermal ratchet models that have been studied, perhaps most famously by Feynman (21, 22). With  $T_2 = 1.5 T_1$  (Fig. 2B), the two simulated time series of random displacements were individually still indistinguishable from equilibrium dynamics. In particular, displacements maintained a Gaussian distribution, even in this nonequilibrium situation (fig. S6) (18). When we applied PFA, however, we found significant probability fluxes in the  $x_1 \times x_2$  plane of CGPS (Fig. 2C). These flux loops demonstrate broken detailed balance, revealing the nonequilibrium nature of the system's dynamics. At equilibrium ( $T_2 = T_1$ ), flux loops vanished (Fig. 2D).

The finite length of time trajectories creates a noise floor in the measured transition rates. To assess the statistical significance of the fluxes determined by PFA, we used trajectory bootstrapping (18, 23). Error estimates are shown as disks centered on flux arrowheads (fig. S2). The comparison with noise demonstrates the statistical significance of fluxes for the nonequilibrium system ( $T_2 = 1.5 T_1$ , Fig. 2C), and their statistical insignificance in equilibrium ( $T_2 = T_1$ , Fig. 2D). The simulations thus demonstrate that even a purely stochastically driven system can be probed for nonequilibrium behavior by detecting broken detailed balance (figs. S4 and S5).

We next turned to a biological system that exhibits a stochastic steady state (18) (figs. S7 to S13). We imaged primary cilia of Madin-Darby canine kidney II (MDCK-II) epithelial cells grown in culture to a confluent layer (Fig. 3A). Primary cilia are hairlike organelles that project from many eukaryotic cells and can transduce mechanical and chemical stimuli into intracellular signals (24). Using invasive biochemical treatments, prior work (25) provided indirect evidence for nonequilibrium dynamics of these cilia. Flagella and primary cilia are structurally related, but the latter often lack the dynein machinery necessary for flagellar beating (26). Indeed, in marked contrast to the flagellum, we found that primary cilia of MDCK cells fluctuate in a way that appears random (Fig. 3B, movie S2, and figs. S14 and S15).

To analyze cilia dynamics, we characterized their state by the average deflection angle  $\theta(t)$  from the normal and the average curvature  $\kappa(t)$  (Fig. 3A) and calculated the probability flux map in the  $\theta \times \kappa$  phase space (Fig. 3, C to E). From the time series  $\theta(t)$  and  $\kappa(t)$  in Fig. 3B (left), we found a clockwise circulation pattern (white box, Fig. 3C), indicative of broken detailed balance. To quantify the statistical robustness of this pattern, we calculated the contour integral along the flux loop (fig. S3) enclosed by the white box (Fig. 3C),  $\Omega = \oint \vec{j} \cdot d\vec{\ell}$ . We found  $\mu_\Omega / \sigma_\Omega = 2.1$ , where  $\mu_\Omega$  and  $\sigma_\Omega$  are the bootstrapped mean and standard deviation of  $\Omega$  (Fig. 3F) (18), indicating a statistically significant flux loop ( $P = 0.018$ , z-test). Long trajectories sometimes exhibited multimodal behavior in the angle

distribution originating from a slow drift in the steady-state angle (Fig. 3G). In such cases, high-pass filtering resulted in a statistically significant clockwise circulation pattern (Fig. 3D) (18). Actin-myosin dynamics underlie many types of cellular dynamics (4, 5, 27, 28), and the cilium basal body is embedded in the actin cortex (Fig. 3A, inset), providing a mechanism for the nonequilibrium motion of the cilium (25, 29, 30). To test whether detailed balance was restored when the main driving force was turned off, we treated MDCK-II cells with blebbistatin, a drug that inhibits nonmuscle myosin II (Fig. 3E). This treatment suppressed the amplitude of angle and curvature fluctuations (Fig. 3B, right), as seen previously (25). The analysis of phase-space trajectories revealed that blebbistatin treatment (Fig. 3E) decreased phase space flux and rendered the residual fluxes statistically insignificant ( $P = 0.16$ ) (Fig. 3F). As a further control, we observed that ATP depletion also suppressed, albeit not completely, cilia fluctuations and strongly decreased the flux pattern in phase space ( $P = 0.16$ ) (fig. S16) (18). Finally, we verified the steady-state nature of cilia dynamics by the vanishing divergence of the fluxes in phase space (fig. S13). Taken together, these results demonstrate that the stochastic dynamics of the cilium can be clearly identified to be of nonequilibrium origin.

Steady-state fluctuations are common in living systems. It has, however, proved challenging to determine whether such stochastic dynamics result from nonequilibrium activity in given cases (3, 11). The PFA approach described here uses commonly observable conformational degrees of freedom to identify nonequilibrium dynamics in steady-state systems. This approach is broadly applicable to active biological systems, ranging from bacteria and the cell nucleus (11), all the way to tissues. Our method is intrinsically noninvasive, being based on imaging alone without requiring biochemical or mechanical manipulation. This is in contrast to other methods, where nonequilibrium fluctuations can be identified by the fluctuation-dissipation theorem or its nonequilibrium generalizations (27, 31). Furthermore, our method does not focus on rare events (32) or transitions between equilibrium states (33–35), nor does it rely on Markovian dynamics (33). It is interesting to consider possible extensions of our method to quantify energy dissipation or entropy production (36).

## Supplementary Material

Refer to Web version on PubMed Central for supplementary material.

## ACKNOWLEDGMENTS

We thank J. Lippincott-Schwartz, U. Seifert, G. Berman, A. El-Hady, B. Machta, and J. Gore for discussions. This research was supported by a Lewis-Sigler fellowship (C.P.B.), the German Excellence Initiative via the program “NanoSystems Initiative Munich” (C.P.B.), and the Cluster of Excellence and Deutsche Forschungsgemeinschaft (DFG) Research Center Nanoscale Microscopy and Molecular Physiology of the Brain (CNMPB) (C.F.S.), a Human Frontier Science Program Fellowship (N.F.), the European Research Council Advanced Grant PF7 ERC-2013-AdG, Project 340528 (C.F.S), the DFG Collaborative Research Center SFB 937 (Project A2), and a research program of the Foundation for Fundamental Research on Matter (FOM), which is part of the Netherlands Organization for Scientific Research (NWO). This work was initiated at the Aspen Center for Physics, which is supported by NSF grant PHY-1066293, and was further supported in part by the NSF under grant NSF PHY11-25915. Experiments with *Chlamydomonas* flagella were performed during the 2011 Physiology Course at the Marine Biological Laboratory, Woods Hole, MA, supported in part by NIH grants R13GM085967 and P50GM068763.

## REFERENCES AND NOTES

1. Boltzmann L, Sitzungsberichte Akad. Wiss., Vienna, part II 66, 275–370 (1872).
2. Alberts B et al., *Molecular Biology of the Cell* (Garland Science, New York, ed. 5 2007).
3. Brangwynne CP, Koenderink GH, MacKintosh FC, Weitz DA, *J. Cell Biol.* 183, 583–587 (2008). [PubMed: 19001127]
4. Fakhri N et al., *Science* 344, 1031–1035 (2014). [PubMed: 24876498]
5. Guo M et al., *Cell* 158, 822–832 (2014). [PubMed: 25126787]
6. Hopfield JJ, *Proc. Natl. Acad. Sci. U.S.A.* 71, 4135–4139 (1974). [PubMed: 4530290]
7. Berg HC, Purcell EM, *Biophys. J.* 20, 193–219 (1977). [PubMed: 911982]
8. Cates ME, *Rep. Prog. Phys.* 75, 042601 (2012). [PubMed: 22790505]
9. Lan G, Sartori P, Neumann S, Sourjik V, Tu Y, *Nat. Phys.* 8, 422–428 (2012). [PubMed: 22737175]
10. Nadrowski B, Martin P, Jülicher F, *Proc. Natl. Acad. Sci. U.S.A.* 101, 12195–12200 (2004). [PubMed: 15302928]
11. Weber SC, Spakowitz AJ, Theriot JA, *Proc. Natl. Acad. Sci. U.S.A.* 109, 7338–7343 (2012). [PubMed: 22517744]
12. Egolf DA, *Science* 287, 101–104 (2000). [PubMed: 10615038]
13. Zia R, Schmittmann B, *J. Stat. Mech.* 2007, P07012 (2007).
14. Purcell EM, *Am. J. Phys.* 45, 3–11 (1977).
15. Riedel-Kruse IH, Hilfinger A, Howard J, Jülicher F, *HFSP J.* 1, 192–208 (2007). [PubMed: 19404446]
16. Wan KY, Goldstein RE, *Phys. Rev. Lett.* 113, 238103 (2014). [PubMed: 25526162]
17. Alper J, Geyer V, Mukundan V, Howard J, *Methods Enzymol.* 524, 343–369 (2013). [PubMed: 23498749]
18. Materials and methods are available as supplementary materials on Science Online.
19. Aragon SR, Pecora R, *Macromolecules* 18, 1868–1875 (1985).
20. Ma R, Klindt GS, Riedel-Kruse IH, Jülicher F, Friedrich BM, *Phys. Rev. Lett.* 113, 048101 (2014). [PubMed: 25105656]
21. Feynman RP, Leighton RB, Sands M, *The Feynman Lectures on Physics*, Vol. 1 (Addison-Wesley, Reading, MA, 1966).
22. Sekimoto K, *J. Phys. Soc. Jpn.* 66, 1234–1237 (1997).
23. Shannon CE, Weaver W, *The Mathematical Theory of Communication* (Univ. of Illinois Press, Urbana, 1949).
24. Singla V, Reiter JF, *Science* 313, 629–633 (2006). [PubMed: 16888132]
25. Battle C, Ott CM, Burnette DT, Lippincott-Schwartz J, Schmidt CF, *Proc. Natl. Acad. Sci. U.S.A.* 112, 1410–1415 (2015). [PubMed: 25605896]
26. Barnes BG, *J. Ultrastruct. Res.* 5, 453–467 (1961). [PubMed: 13865089]
27. Mizuno D, Tardin C, Schmidt CF, Mackintosh FC, *Science* 315, 370–373 (2007). [PubMed: 17234946]
28. Brangwynne CP, Koenderink GH, Mackintosh FC, Weitz DA, *Phys. Rev. Lett.* 100, 118104 (2008). [PubMed: 18517833]
29. Antoniadis I, Stylianou P, Skourides PA, *Dev. Cell* 28, 70–80 (2014). [PubMed: 24434137]
30. Marshall WF, *Curr. Top. Dev. Biol.* 85, 1–22 (2008). [PubMed: 19147000]
31. Prost J, Joanny JF, Parrondo JM, *Phys. Rev. Lett.* 103, 090601 (2009). [PubMed: 19792774]
32. Bustamante C, Liphardt J, Ritort F, *Phys. Today* 58, 43–48 (2005).
33. Crooks GE, *Phys. Rev. E Stat. Phys. Plasmas Fluids Relat. Interdiscip. Topics* 60, 2721–2726 (1999). [PubMed: 11970075]
34. Jarzynski C, *Phys. Rev. Lett.* 78, 2690–2693 (1997).
35. Liphardt J, Dumont S, Smith SB, Tinoco I Jr., Bustamante C, *Science* 296, 1832–1835 (2002). [PubMed: 12052949]
36. Seifert U, *Phys. Rev. Lett.* 95, 040602(2005). [PubMed: 16090792]

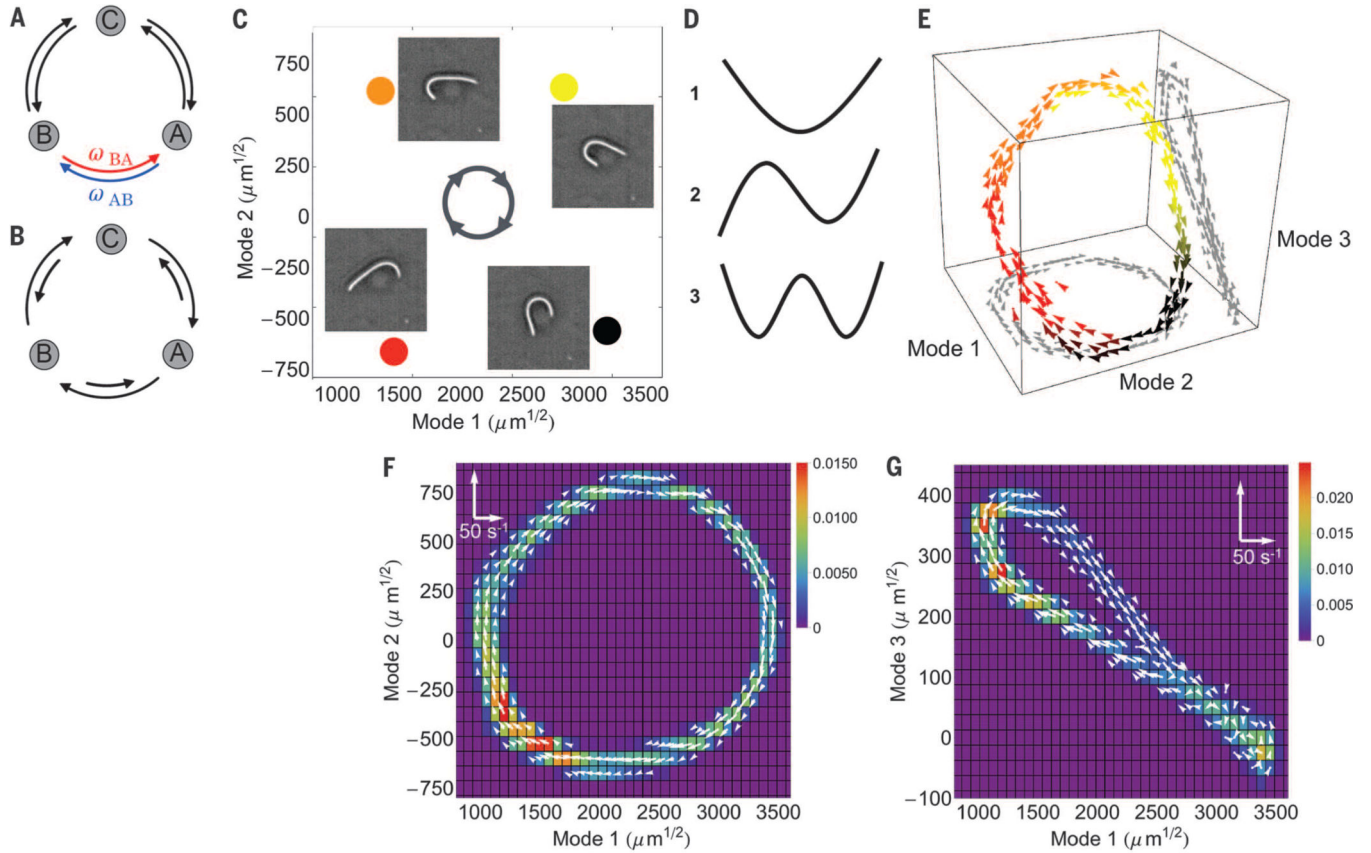


**Fig. 1. Detailed balance and actively beating *Chlamydomonas* flagella.**

(A) In thermodynamic equilibrium, transitions between microscopic states are pairwise-balanced, precluding net flux among states. (B) Nonequilibrium steady states can break detailed balance and exhibit flux loops. (C) Snapshots separated by 24 (orange-yellow), 7, and 10 ms in an isolated *Chlamydomonas* flagellum's beat cycle (movie S1). Arrows on the central circle indicate the direction of time. Color corresponds to position in (E). (D) The first three bending modes for a freely suspended flexible rod. (E) A three-dimensional (3D) probability flux map of flagellar dynamics in the CGPS spanned by the first three modes. (F and G) Probability distribution (color) and flux map (white arrows) of flagellar dynamics in CGPS spanned by first and second modes (F), and first and third modes (G). The white legend indicates the flux scale.

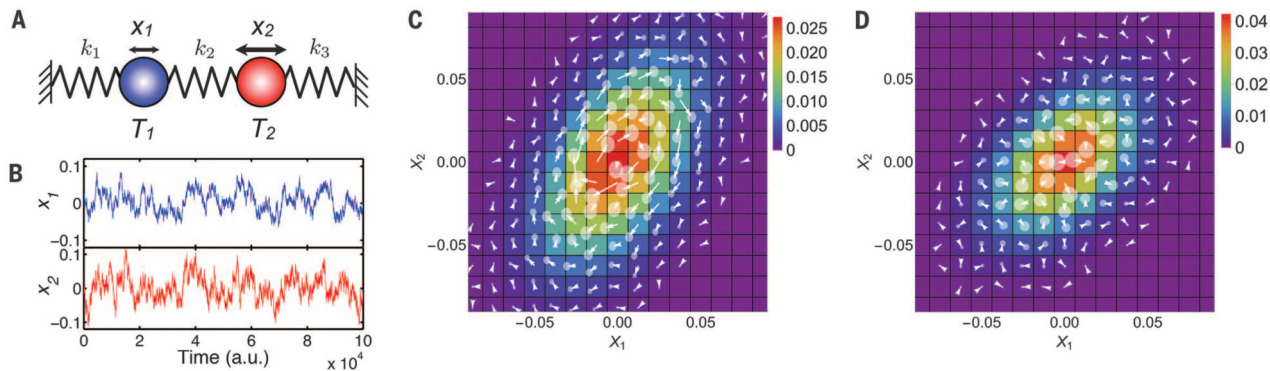


**Fig. 2. Brownian-dynamics simulation of 1D bead-spring model.**

(A) Model schematic. (B) Time series of the bead positions for  $T_2 = 1.5T_1$  and equal spring constants. See figs. S4 and S5 for the general case (18). (C and D) Probability distribution (color) and flux map (white arrows) in CGPS spanned by  $x_1$  and  $x_2$  for the simulation in panel B (C) and for a simulation with  $T_2 = T_1$  (D). Translucent disks represent a  $2\sigma$  confidence interval for fluxes.

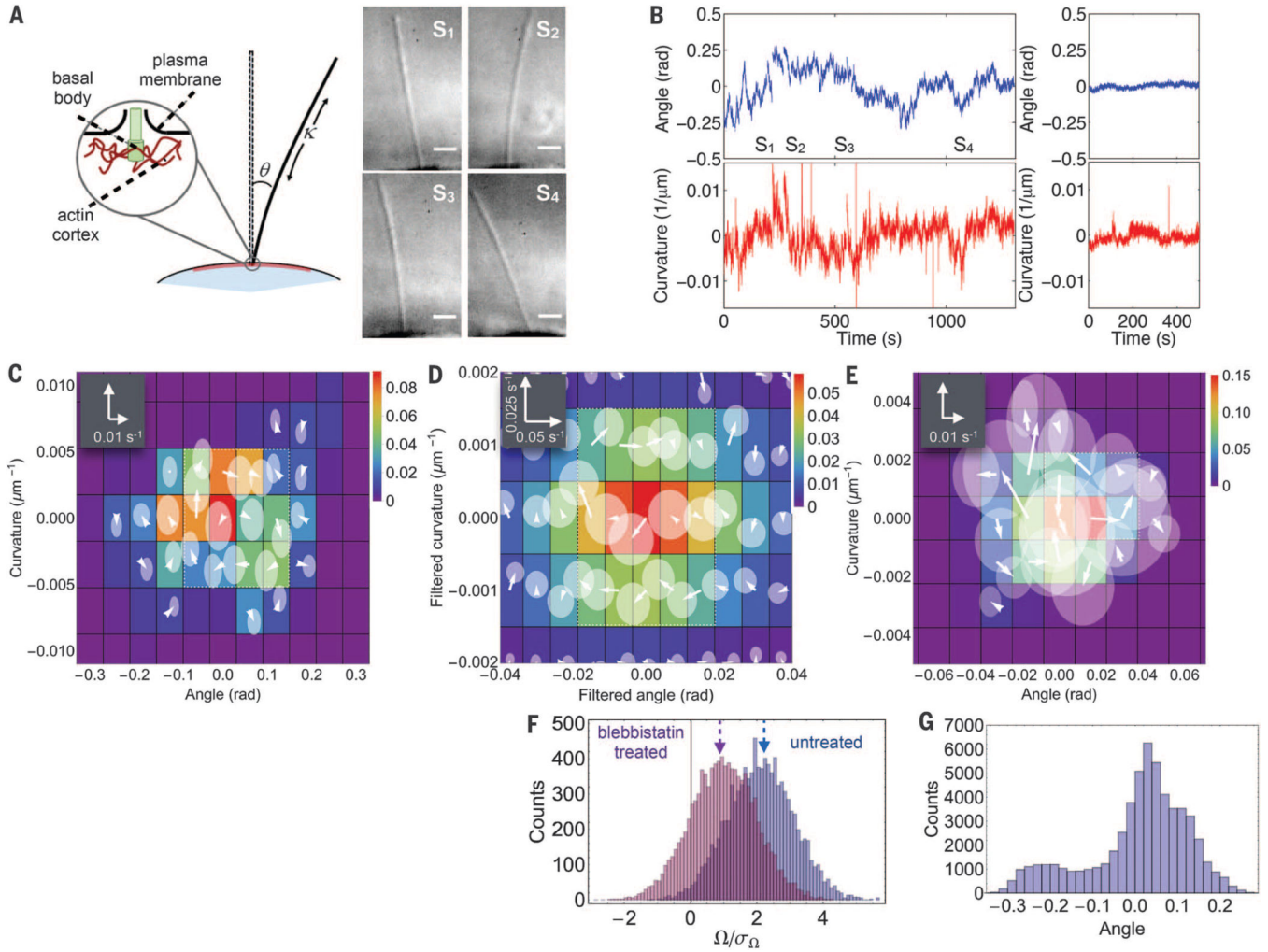


**Fig. 3. Nonequilibrium fluctuations of MDCK-II primary cilia.**

(A) Left: Schematic of primary cilium and anchoring of the basal body in the cell cortex with angle  $\theta$  and curvature,  $\kappa$ , defined positive as shown. Right: Snapshots of cilium, from differential interference contrast microscopy, taken at time points marked in (B). Scale bar: 2  $\mu\text{m}$ . (B) Angle (top) and curvature time series (bottom) of an active cilium (left) and of a blebbistatin-treated cilium (right). Frame rate: 25 Hz; scale bar: 2  $\mu\text{m}$ . (C to E) Phase-space probability distribution (color) and flux map (white arrows) of ciliary fluctuations in CGPS spanned by  $\theta$  and  $\kappa$  for (C): the untreated time series from (B); (D) a high-pass filtered time series of an untreated cilium (window size = 200 s); (E) the fluctuations of the blebbistatin-treated cilium from (B). The translucent disks represent a  $2\sigma$  confidence interval for fluxes. (F) Distributions of flux contour integrals for untreated (purple) and blebbistatin-treated (pink) cilia. (G) Angle distribution for the high-pass filtered cilium data in (D).